Anal Bioanal Chem (2014) 406:7037–7046
DOI 10.1007/s00216-014-7927-0

RESEARCH PAPER

Complexity of fatty acid distribution inside human macrophages on single cell level using Raman micro-spectroscopy

Clara Stiebing · Christian Matthäus · Christoph Krafft · Andrea-Anneliese Keller · Karina Weber · Stefan Lorkowski · Jürgen Popp

Received: 31 March 2014 / Revised: 26 May 2014 / Accepted: 26 May 2014 / Published online: 18 June 2014

Abstract Macrophages are phagocytic cells which are involved in the non-specific immune defense. Lipid uptake and storage behavior of macrophages also play a key role in the development of atherosclerotic lesions within walls of blood vessels. The allocation of exogenous lipids such as fatty acids in the blood stream dictates the accumulation and quantity of lipids within macrophages. In case of an overexposure, macrophages transform into foam cells because of the large amount of lipid droplets in the cytoplasm. Raman microspectroscopy is a powerful tool for studying single cells due to the combination of microscopic imaging with spectral information. With a spatial resolution restricted by the diffraction limit, it is possible to visualize lipid droplets within macrophages. With stable isotopic labeling of fatty acids with deuterium, the uptake and storage of exogenously provided fatty acids can be investigated. In this study, we present the results of time-dependent Raman spectroscopic imaging of single THP-1 macrophages incubated with deuterated arachidonic acid. The polyunsaturated fatty acid plays an important role in the cellular signaling pathway as being the precursor of icosanoids. We show that arachidonic acid is stored in lipid droplets but foam cell formation is less pronounced as with other fatty acids. The storage efficiency in lipid droplets is lower than in cells incubated with deuterated palmitic acid. We validate our results with gas chromatography and gain information on the relative content of arachidonic acid and its metabolites in treated macrophages. These analyses also provide evidence that significant amounts of the intracellular arachidonic acid is elongated to adrenic acid but is not metabolized any further. The co-supplementation of deuterated arachidonic acid and deuterated palmitic acid leads to a non-homogenous storage pattern in lipid droplets within single cells.

Keywords Macrophages · Lipid droplet · Arachidonic acid · Atherosclerosis · Gas chromatography · Raman spectroscopy

Stefan Lorkowski and Jürgen Popp contributed equally to this work.

Published in the topical collection *Single Cell Analysis* with guest editors Petra Dittrich and Norbert Jakubowski.

Electronic supplementary material The online version of this article (doi:10.1007/s00216-014-7927-0) contains supplementary material, which is available to authorized users.

C. Stiebing · C. Matthäus · C. Krafft · K. Weber · J. Popp (✉)
Leibniz Institute of Photonic Technology (IPHT),
Albert-Einstein-Straße 9, 07745 Jena, Germany
e-mail: juergen.popp@ipht-jena.de

C. Stiebing · C. Matthäus · C. Krafft · K. Weber · J. Popp
Institute of Physical Chemistry and Abbe Center of Photonics,
Friedrich Schiller University Jena, Helmholtzweg 4, 07743 Jena,
Germany

A.-A. Keller · S. Lorkowski
Institute of Nutrition and Abbe Center of Photonics, Friedrich
Schiller University Jena, Dornburger Straße 25, 07743 Jena,
Germany

Introduction

Macrophages are involved in the non-specific immune response. They take up various biological materials, such as lipids, bacteria or debris. Lipid uptake and storage behavior of macrophages play a key role in the development of atherosclerotic lesions within the walls of blood vessels. Macrophages are monocyte-derived cells which are often located in the subendothelial area of arteries in case of local damage or inflammation. Through receptor-mediated pathways, macrophages take up lipids complexed in lipoproteins as well as fatty acids bound to serum albumin in the blood stream. Both processes are uncontrolled leading to tremendous accumulation of lipids inside the cell in form of cytosolic lipid droplets. Eventually, extensive formation of lipid droplets leads to a

foamy appearance of the cells, called foam cell formation, but also toxic levels are reached upon excessive uptake. Apoptosis or necrosis takes place and the excessive lipid content of the macrophage is released into the arterial walls, where the lipid depositions consequently form atherosclerotic plaques [1].

Lipid droplets are very interesting dynamic cellular organelles. Although plenty of research has been conducted, there are still various questions about the development and composition of lipid droplets [2, 3]. Many studies involve the incubation of different cell types with fatty acids, as for instance the saturated palmitic acid or monounsaturated oleic acid, to study their lipotoxicity and storage characteristics [4, 5]. Common methods to investigate lipid droplets are biochemical fractionation, gas chromatography, also combined with mass spectrometry, electron microscopy and fluorescence microscopy. Raman micro-spectroscopy, as a vibrational spectroscopic imaging method, has recently gained popularity to identify cells and study cellular processes [6–17]. A Raman spectrum is a representation of all chemical components present in the laser focus. With a spatial resolution restricted by the diffraction limit, Raman micro-spectroscopy provides the possibility to correlate the visual image of cells with chemical information.

Schie et al. evaluated the concentration of palmitic acid and oleic acid in lipid droplets by comparing Raman spectra of lipid droplets of hepatocytes to pure component spectra by using least square fitting algorithms [18]. Their results showed that asymmetric least square fitting is a very feasible possibility to analyze the content of individual lipid droplets in cells, which is independent of external labels. However, without any labeling, it is not possible to distinguish exogenously added fatty acids from the cell-intrinsic fatty acids. Macrophages, especially, can exhibit many lipid droplets under culture conditions in the presence of serum before any incubation and hence contain a variety of endogenous cellular lipids. To ascertain that a fatty acid is taken up by the cell and stored in lipid droplets, deuterium labels can be introduced [19–22]. Due to the higher mass of deuterium than hydrogen, deuterium-associated vibrational bands are shifted to lower wavenumbers compared to hydrogen bands. CH stretching vibrations exhibit spectral contributions around 2,800–3,100 cm^{-1} and significantly shift to 2,000–2,500 cm^{-1} through the exchange of hydrogen with deuterium. Therefore, CD stretching vibrations have spectral contributions within a normally silent region. Furthermore, band shifts of CD vibrations between pure spectra and lipid spectra inside of lipid droplets can be interpreted as a clear indication for structural changes.

With FTIR micro-spectroscopy, Gazi et al. studied the effect of deuterated palmitic acid, as well as deuterated arachidonic acid on exposed prostate cancer cells (PC-3) [23]. In an earlier study the group showed that PC-3 cells translocate lipids with adipocytes, which were previously incubated with deuterated palmitic acid [24]. The study demonstrates nicely the power of isotopic labeling with deuterium by tracking the signal originating through deuterium bond vibrations. However, due to the longer wavelength used in FTIR microspectroscopy, the spatial resolution is inferior to Raman microscopy and single lipid droplets of non-adipocytes cannot be resolved.

Apparently, compositional parameters can have great influence on lipotoxicity. Co-supplementation studies by Listenberger et al. have been conducted using oleic acid and palmitic acid to investigate fatty acid induced cell death [4]. The study showed that in Chinese hamster ovary (CHO) cells, oleic acid channels palmitic acid to triglyceride storage when given supplementary. Solely added, incubation with palmitic acid caused apoptosis through lipotoxicity. It has been shown that triglyceride storage protects against lipotoxicity and that triglyceride accumulation is higher in cells treated with polyunsaturated fatty acids. These findings were confirmed by Martins de Lima et al. [5], who performed lipotoxicity tests on J774.A1 macrophages with different types of fatty acids including palmitic acid, oleic acid and arachidonic acid. These studies indicated that the toxicity of fatty acids is not strictly related to carbon-chain length and the number of double bonds.

The polyunsaturated arachidonic acid is an essential omega-6-fatty acid and acts as a bioactive molecule [25, 26]. It plays an important role for inflammatory signaling in cells as the precursor of icosanoids. Arachidonic acid can be esterified and stored in cellular lipid compartments besides its use in phospholipids such as phosphatidylethanolamine, phosphatidylcholine, and phosphatidylinositides [27]. Van Manen et al. used deuterated arachidonic acid to investigate the association of lipid bodies with phagosomes in leukocytes [28]. They showed that incubation with arachidonic acid leads to esterified arachidonate in the lipid bodies near the phagocytized microspheres.

In this study, we present the results of time-dependent Raman spectroscopic imaging of single THP-1 macrophages incubated with deuterated arachidonic acid. Through data analyses with a spectral unmixing algorithm, we found that deuterated arachidonic acid is stored in lipid droplets but less efficiently than deuterated palmitic acid and oleic acid as previously shown [19]. The Raman spectroscopic imaging results were compared to gas chromatographic analyses. We observed a significant increase of arachidonic acid but also adrenic acid as the first two-carbon elongation product of arachidonic acid in the macrophages during the incubation process. The co-supplementation of deuterated arachidonic acid and palmitic acid lead to non-homogeneous storage in lipid droplets within a single cell. To the best of our knowledge, non-homogeneous storage patterns of two different types of fatty acids in lipid droplets of one cell have not yet been shown.

Material and methods

Cell culture

THP-1 monocytes (DSMZ, Braunschweig, Germany) have been cultured in RPMI 1640 medium (Sigma-Aldrich, St. Louis, MO) containing 10 % (*v*/*v*) fetal bovine serum superior (Biochrom, Berlin) and 1 % (*v*/*v*) penicillin/streptomycin/L-glutamine (Sigma-Aldrich) in an atmosphere of 5 % CO_2 at 37 °C. Monocytes have been differentiated into macrophages using RPMI 1640 medium supplemented with 100 ng/mL phorbol-12-myristate-13-acetate and 50 μM β-mercaptoethanol for 96 h as previously described [29, 30]. After differentiation, mature THP-1 macrophages were incubated for up to 32 h. Supplemented RPMI 1640 medium without serum was used with either 400 μM d_8-arachidonic acid or a mixture of 400 μM d_8-arachidonic acid and 400 μM d_{31}-palmitic acid (Sigma-Aldrich). Before incubation, the fatty acids were complexed to fatty acid-free bovine serum albumin (Sigma-Aldrich) at a molar ratio of 4:1 in Krebs-Ringer bicarbonate buffer. After incubation, cells were washed with phosphate buffered saline (PBS) and fixed with 4 % (*w*/*v*) paraformaldehyde in PBS for 20 min at room temperature.

Raman measurements

For Raman imaging, THP-1 macrophages were grown on calcium fluoride slides (Crystal, Berlin, Germany), in order to avoid disturbing background signals caused by common glass slides. Raman images were acquired using a confocal Raman Microscope Model alpha300 R (WITec, Ulm, Germany) and a Nikon water immersion objective with a magnification of ×60 and a numerical aperture of 1.00. An excitation wavelength of 785 nm was provided by a cw diode laser (Toptica Photonics, Gräfelingen, Germany). Raman images were taken at a step size of 0.5 μm with an integration time of 0.5 s. Each pixel in an image represents one spectrum. If not declared otherwise, a grating of 300 grooves/mm was used, leading to a spectral resolution of around 6 cm^{-1}.

Data analysis of Raman measurements

All spectra were cleared from cosmic rays before analysis using the software CytoSpec (Cytospec, Berlin, Germany). Image analysis and spectral quantification was then performed in MatLab (MathWorks, Natick, MA). Baseline correction with a second order polynomial and vector normalization was implemented. Images acquired with Raman microspectroscopy were analyzed by the N-FINDR spectral unmixing algorithm described by Winter et al. [31, 32]. A wavenumber region from 500 to 3,100 cm^{-1} was used. The quantification of d_8-arachidonic acid was performed by an asymmetric least square fitting [33, 18]. A wavenumber region of 1,900 to 2,500 cm^{-1} was chosen to evaluate the uptake of d_8-arachidonic acid through the deuterium signal in lipid droplets. Graphs were plotted and evaluated in Origin (OriginLab, Northampton, MA).

Gas chromatography

Lipids were extracted from mature THP-1 macrophages cultured for the times indicated in the figures with serum albumin-complexed fatty acids using a methanol/chloroform/water-mixture (2:1:1, *v*/*v*/*v*) according to the method of Bligh and Dyer [34]. Fatty acid methyl esters (FAME) were prepared with boron trifluoride in methanol (10 %, *v*/*v*; Supelco, Bellefonte, PA). Fatty acid analyses were conducted by gas chromatography using a Shimadzu GC-17V3 (Tokyo, Japan) equipped with auto sampler and flame ionization detector. Fatty acids ranging from 4 to 26 carbon atoms in length were determined using a fused silica capillary column (DB-225 ms: 60 m, i.d. 0.25 mm, 0.25 mm film thickness; Agilent Technologies, Böblingen, Germany). Analysis of *trans* fatty acids were conducted by a second measurement using a Shimadzu GC-2010 with flame ionization detector and a high polarity column (CP 7421: 200 m, i.d. 0.25 mm, 0.25 μm film thickness; Varian, Middelburg, the Netherlands). Various reference standards were used as FAME mix to verify the identity of fatty acid peaks: No. 463, 674 (NU-CHEK PREP, Elysian, MN), BR2, BR4, and ME 93 (Larodan, Sweden), Menhaden and several *cis*/*trans* standards (Supelco). Peaks of C24:4 (*n*−6) and C24:5 (*n*−6) were located by extrapolation as no standards were available. LabSolutions software for gas chromatography (GCsolution, Shimadzu, Japan) was used for peak integration. The measurements were recalculated with each other under consideration of the respective response factor. Fatty acid concentrations are expressed as percentage of the total area of all FA peaks (% of total FAME). The procedure was adapted from Kraft et al. [35].

Results and discussion

Uptake and storage of d_8-arachidonic acid by THP-1 macrophages

Figure 1a shows the Raman spectrum of pure d_8-arachidonic acid. The molecule is deuterated at eight positions as depicted in Fig. 1a. Deuterium labels are introduced at carbon atoms which feature a double bond. A specific signal between 2,100 and 2,300 cm^{-1} appears due to =CD stretching vibrations in the usually silent region of non-deuterated fatty acid spectra. The spectrum is dominated by the band at 1,633 cm^{-1} which corresponds to Raman scattering intensities of C=C bonds.

Due to the deuterium label, the band appears at a lower wavenumber instead of around 1,655 cm^{-1} reported for non-deuterated, unsaturated fatty acids [11, 28, 36].

The bright field image of a macrophage incubated with 400 μM d_8-arachidonic acid complexed to serum albumin for 24 h is shown in Fig. 1b. The cytosolic lipid droplets are located close to the nucleus which contains a clearly visible nucleolus. Raman micro-spectroscopic images of treated cells were analyzed using the N-FINDR algorithm. The output spectra, usually referred to as endmembers, can be interpreted as spectra which represent the highest differences in the hyperspectral dataset. The number of used endmembers was chosen so that the protein and lipid composition could be differentiated. In average, this led to three endmembers—one corresponding to lipids, one to proteins and one to the cell surrounding background (see Electronic Supplementary Material Fig. S1). Using more endmembers proved to be not beneficial, e.g., having more than one spectrum corresponding to lipids resulted only in a change of overall intensity. Therefore, the two main components represented by endmember spectra for the cell in Fig. 1b are the lipid (red) and protein (cyan) distribution within the cell (Fig. 1c), which were used to reconstruct the false-color image depicted in Fig. 1d. In the red spectrum, the deuterium signal is clearly visible between 2,100 and 2,300 cm^{-1}, providing evidence that d_8-arachidonic acid is taken up and stored in lipid droplets of THP-1 macrophages. The fingerprint region between 500 and 2,000 cm^{-1} exhibits typical spectral characteristics of lipids and corresponds to a composition of different fatty acids within the lipid droplets. The shift of the C═C band from 1,633 to 1,640 cm^{-1} and the C═O band of ester groups at 1,743 cm^{-1} that is not present in Fig. 1a indicate that non-deuterated lipids are also part of the lipid droplets in addition to deuterated arachidonic acid. Figure 1d shows the corresponding,

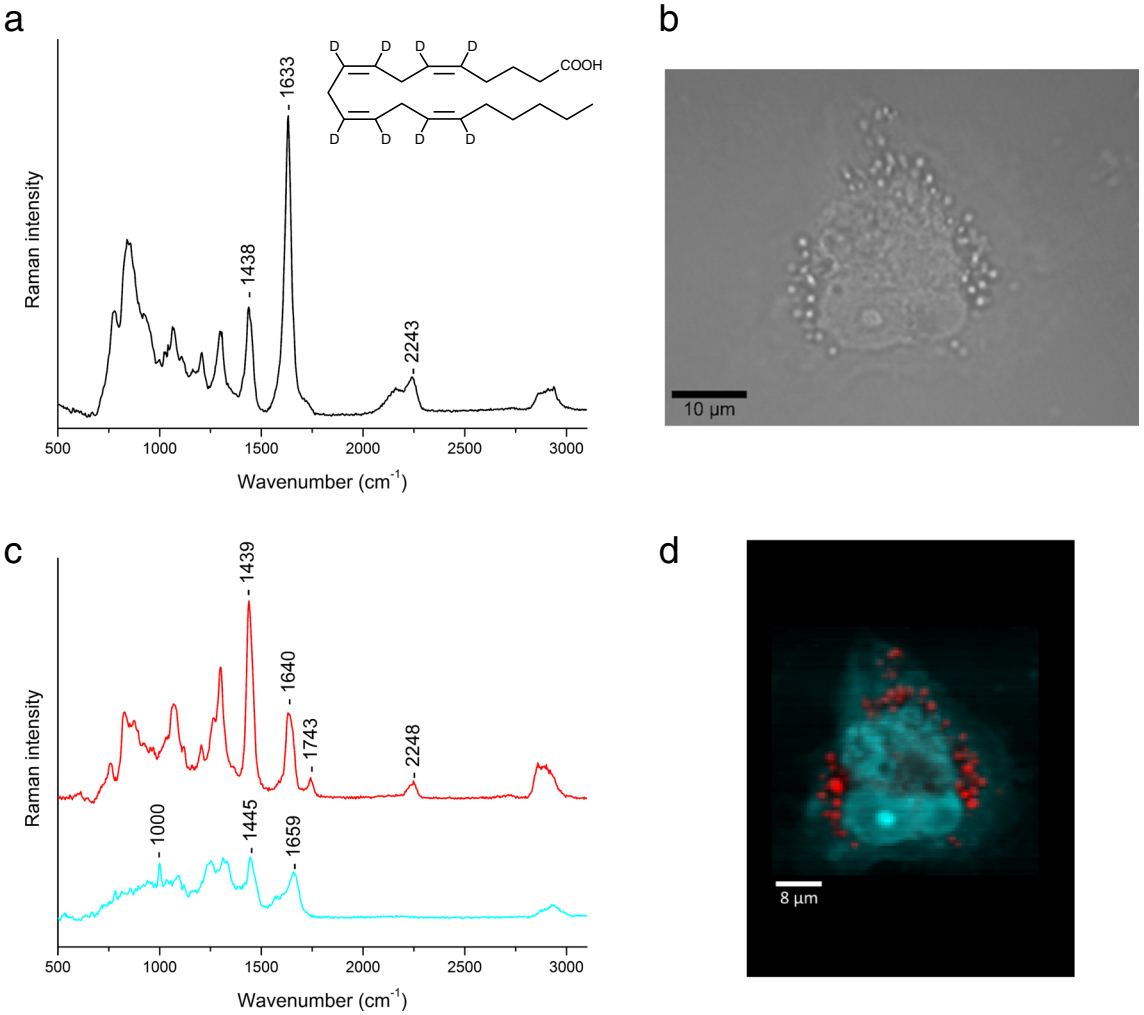

Fig. 1 **a** Chemical structure and Raman spectrum of pure d_8-arachidonic acid. The spectral features between 2,100 and 2,300 cm^{-1} originate from ═CD stretching vibrations. **b** Bright field image of a THP-1 macrophage incubated with 400 μM d_8-arachidonic acid complexed to serum albumin for 24 h. **c** Raman endmember spectra of the imaged cell in **b** after applying the N-FINDR algorithm showing the lipid composition including the deuterium signal of d_8-arachidonic acid in *red* and the protein composition in *cyan*. **d** Reconstructed cell image after N-FINDR analysis of **b**. The *colors* correspond to the endmember spectra in **c**

reconstructed image. The color intensity corresponds to the density and concentration of the plotted components. The nucleus and nucleolus are distinguishable due to the higher protein density compared to the cytoplasm. The lipid droplets with a diameter from 0.5 to 2 μm are clearly visible and colored in red. Smaller lipid accumulations are difficult to resolve due to the resolution limit.

Although arachidonic acid is a biologically active fatty acid, our results show clearly that it is stored in lipid droplets in case of excessive exposure of the cells. By enhancing the spectral resolution from approximately 6 to 3 cm^{-1} by using a grating of 600 grooves/mm, the band corresponding to C=C stretching vibrations features two maxima at 1,633 and 1,653 cm^{-1} (as shown below). This suggests that the double bonds of d_8-arachidonic acid are not oxidized during their accumulation in lipid droplets.

To investigate the time-dependent uptake of d_8-arachidonic acid into THP-1 macrophages different incubation times were chosen. Reconstructed cell images based on the N-FINDR analysis are shown in Fig. 2. The first column shows control cells which were fixed after the differentiation process without any incubation with fatty acids. Here, lipid droplets do not show deuterium signals (depicted in blue) and differ in quantity inside individual cells. Monocytes cannot be synchronized in the way that they are in the same cell cycle phase before the differentiation process begins. Hence, macrophages show large inter-cell variability and already exhibit highly different amounts of lipid droplets prior to incubation with serum albumin-complexed fatty acids. After 3 h of incubation, a clear deuterium signal of the d_8-arachidonic acid appears in the spectra corresponding to lipid droplets (depicted in red). A quantification of d_8-arachidonic acid in lipid droplets was performed through an asymmetric least square fitting of the endmember spectra corresponding to lipids for each cell and time point compared to the pure d_8-arachidonic acid spectrum. A wavenumber region between 1,900 and 2,500 cm^{-1} was chosen to only investigate bands originating from deuterium bond vibrations of d_8-arachidonic acid. In the lower wavenumber region, overlapping spectral contributions of all fatty acids within a droplet are present. Figure 3 displays the results for all measured cells plotted over the incubation time. A rapid increase of d_8-arachidonic acid in lipid droplets is occurring initially but after 3 h of incubation storage capacity is nearly exploited. Saturation is reached after 8 h. A high variation of the quantification for each time point was observed, which can be attributed to the non-synchronized cell cultivation protocol mentioned earlier.

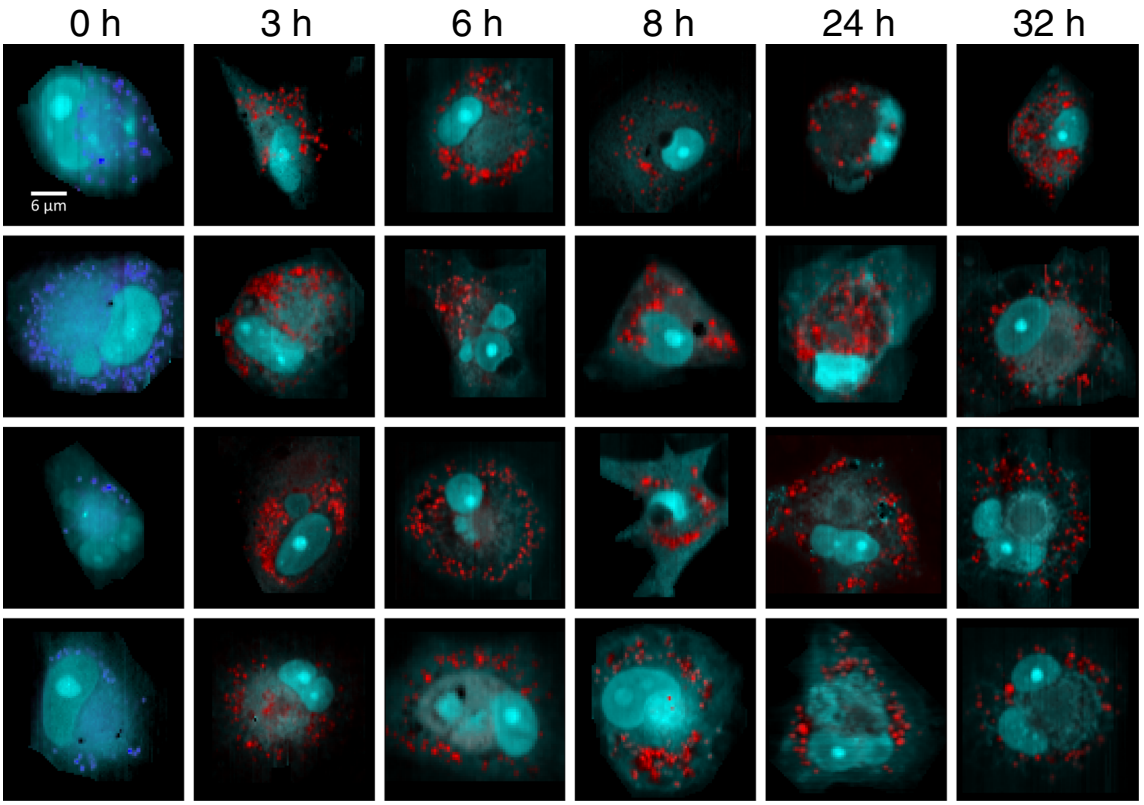

Fig. 2 Time-dependent series of incubated THP-1 macrophages with d_8-arachidonic acid complexed to serum albumin at a concentration of 400 μM. The time points are indicated at the top of the columns. Images were reconstructed based on the lipid and protein endmember spectra after N-FINDR analysis of the measured cells. At 0 h, no deuterium signals in the lipid component (*blue*) and hence no d_8-arachidonic acid was detected. Over time, the deuterium signal in the lipid endmember spectra (*red*) is increasing. The protein distribution is depicted in *cyan*

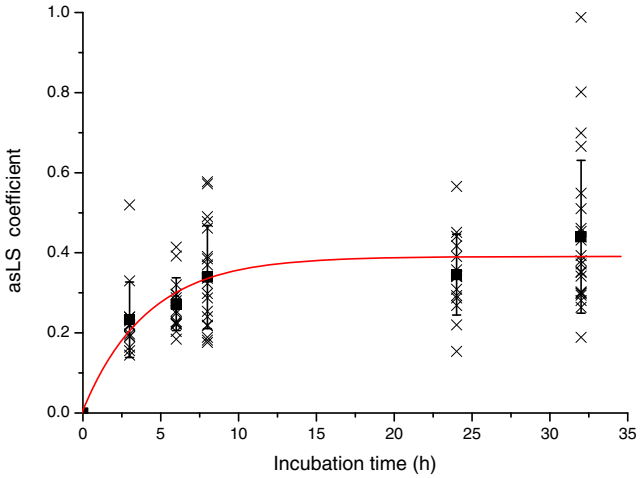

Fig. 3 Quantification of the uptake and storage of d_8-arachidonic acid into lipid droplets over time using an asymmetric least square (*asLS*) fitting of the endmember spectra corresponding to lipids to the pure d_8-arachidonic acid spectrum between 1,900 and 2,500 cm^{-1}. A quick uptake and storage in lipid droplets is detected. Saturation is reached after 8 h. *Cross* single cell measurement; *box* averaged value for each time point; *red line* fitted saturation curve

Over time, the content of d_8-arachidonic acid in lipid droplets is increasing. However, no foam cell formation is visible as no apparent excess of lipid droplets inside the cell's cytoplasm occurs. This is in contrast to previous experiments conducted on saturated palmitic and unsaturated oleic acid, where clear foam cell formation was detected after 24 h of incubation [19]. The storage of arachidonic acid in lipid droplets is therefore less efficient. Our findings indicate that this fatty acid is not only stored in lipid droplets but also metabolized or subjected to other cellular compartments, for example, in form of phospholipids.

GC analysis of macrophages after arachidonic acid uptake

To confirm and extend the results obtained by Raman microspectroscopy, gas chromatographic analyses of THP-1 macrophages cultured in the presence of 400 μM arachidonic acid complexed to serum albumin for the times indicated in Fig. 4 were performed. In contrast to the Raman measurements, gas chromatography investigates bulk samples and therefore the total amount of cellular fatty acids without spatial information. In addition to the relative content of different types of fatty acids it is possible to obtain information on the metabolic fate of individual fatty acids, such as shortening by β-oxidation, elongation, and desaturation.

Figure 4 displays the relative content of arachidonic acid (C20:4) as well as its metabolic precursor dihomo-γ-linolenic acid (C20:3) and its metabolites adrenic acid (C22:4) and tetracosatetraenoic acid (C24:4) inside of arachidonic acid treated THP-1 macrophages. This information is supplemented by Table 1 which provides the numeric data shown in Fig. 4 plus data on the remaining fatty acids of the metabolic pathway, namely the precursors linoleic acid (C18:2) and γ-linolenic acid (C18:3), and the metabolites tetracosapentaenoic acid (C24:5) and docosapentaenoic acid (C22:5). The total fatty acid content at each time point corresponds to 100 %. Chemical structures and the metabolic interactions between these fatty acids are displayed in Fig. 5. As expected, arachidonic acid is rapidly taken up by macrophages. Its cellular content increases steadily over time but slows down towards longer periods of incubation reaching a plateau after 12 h. After 24 h of incubation the relative cellular amount of arachidonic acid is about 50 %. In addition, a relevant increase of adrenic acid as the first two-carbon elongation product of arachidonic acid is also detected. Without reaching a plateau the cellular content of adrenic acid steadily increases up to nearly 16 % after 24 h whereas the cellular content of the next two-carbon elongation product tetracosatetraenoic acid increases only slightly. After 24 h its cellular content is less than 2 %. The subsequent metabolites likely produced by the pathway analogous to the Sprecher's shunt via desaturation (tetracosapentaenoic acid) and subsequent β-oxidation (docosapentaenoic acid) comprised each less than 0.1 % of the total cellular content.

Saturation of macrophage uptake of arachidonic acid is later than saturation of the storage of arachidonic acid in lipid droplets. This indicates that arachidonic acid is first stored in lipid droplets where saturation is reached after 8 h. For longer incubation times, the fatty acid is more likely incorporated into phospholipids of cell and organelle membranes. Raman spectroscopy only allows identifying components of a certain local concentration and size. Single arachidonic acid

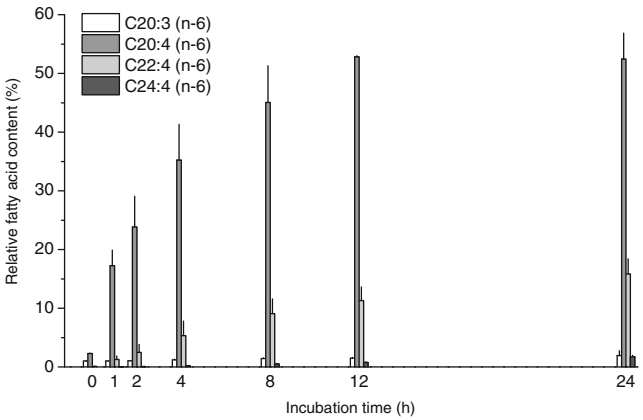

Fig. 4 Time-dependent results of THP-1 macrophages incubated with 400 μM arachidonic acid (C20:4) obtained by gas chromatography. The relative fatty acid content of arachidonic acid (C20:4) and its metabolic precursor dihomo-γ-linolenic acid (C20:3) and its metabolites adrenic acid (C22:4) and tetracosatetraenoic acid (C24:4) are displayed. The total fatty acid content at each time point corresponds to 100 %. A rapid increase of relative arachidonic acid content inside of macrophages is observed and saturation is reached after 12 h. Adrenic acid as the first two-carbon elongation product of arachidonic acid appears during the incubation with arachidonic acid and reaches 16 % of relative fatty acid content in the cells after 24 h. Numeric data is provided in Table 1

Table 1 Percentage of total fatty acid content in THP-1 macrophages after different times of incubation with 400 μM arachidonic acid complexed to serum albumin obtained by gas chromatography. Only fatty acids metabolized from arachidonic acid and directed to the Sprecher's shunt as well as the metabolic precursors of arachidonic acid are shown

s	*n*−6	0 h	1 h	2 h	4 h	8 h	12 h	24 h
Linoleic acid	C18:2 all-*cis*-9,12	1.45±0.13	1.29±0.08	1.17±0.01	0.94±0.02	0.71±0.07	0.56±0.00	0.46±0.03
γ-Linolenic acid	C18:3 all-*cis*-6,9,12	0.00±0.00	0.08±0.01	0.11±0.03	0.17±0.04	0.24±0.06	0.32±0.02	0.49±0.05
Dihomo-γ-linolenic acid	C20:3 all-*cis*-8,11,14	1.00±0.03	1.02±0.07	1.05±0.06	1.20±0.15	1.43±0.11	1.50±0.11	1.94±0.81
Arachidonic acid	C20:4 all-*cis*-5,8,11,14	2.28±0.06	17.24±2.68	23.83±5.24	35.25±6.07	45.04±6.26	52.84±0.18	52.45±4.42
Adrenic acid	C22:4 all-*cis*-7,10,13,16	0.11±0.03	1.26±0.60	2.47±1.37	5.33±2.48	9.08±2.52	11.30±2.32	15.85±2.58
Tetracosatetraenoic acid	C24:4 all-*cis*-9,12,15,18	0.00±0.00	0.03±0.00	0.05±0.02	0.21±0.09	0.52±0.09	0.77±0.10	1.73±0.25
Tetracosapentaenoic acid	C24:5 all-*cis*-6,9,12,15,18	0.00±0.00	0.00±0.00	0.00±0.00	0.00±0.00	0.01±0.01	0.01±0.01	0.03±0.03
Docosapentaenoic acid	C22:5 all-*cis*-4,7,10,13,16	0.03±0.01	0.02±0.02	0.02±0.03	0.01±0.02	0.02±0.01	0.02±0.02	0.03±0.01

molecules or the arachidonic acid-containing phospholipids in cellular membranes cannot be detected by Raman microspectroscopic imaging. Further investigations have to be conducted whether arachidonic acid is stored unaltered in lipid droplets or rather elongated and stored as adrenic acid. The reason for the elongation may be that it is energetically more favorable to store longer fatty acid chains or that it protects the cells from an overexposure with arachidonic acid thus

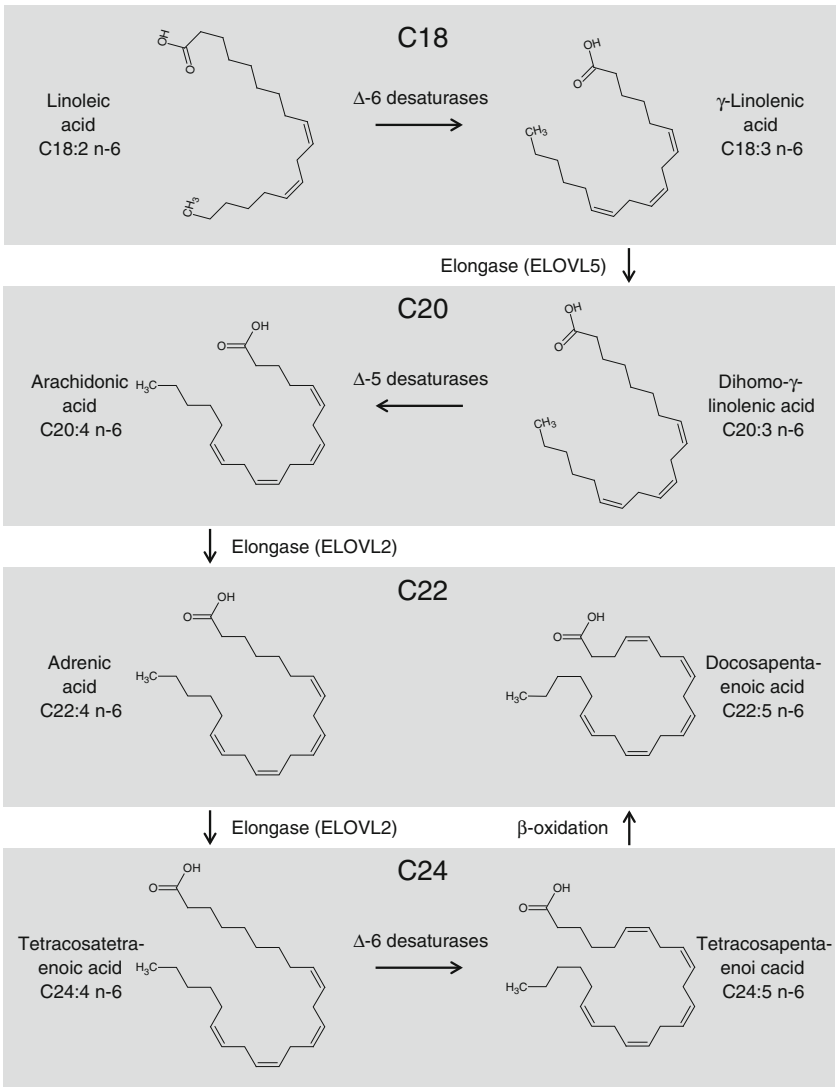

Fig. 5 Chemical structures of the fatty acids listed in Table 1 including their metabolic interactions. The number of carbon atoms increases downwards. *Arrows* depict the interactions between the fatty acids

hindering an overproduction of icosanoids. Comai et al. investigated isolated lipid droplets from rabbit renal medullary tissue and showed that adrenic and arachidonic acid are both present as triglycerides in cytosolic lipid droplets [37]. The difference of two carbons does not change the chemical structure sufficiently to detect intensity or wavenumber variations in Raman spectra between adrenic and arachidonic acid and we therefore cannot deduce which type of fatty acid is more prominent in lipid droplets.

Colocalization of d_8-arachidonic acid and d_{31}-palmitic acid in THP-1 macrophages

For Raman measurements, THP-1 macrophages were treated simultaneously with d_8-arachidonic acid and d_{31}-palmitic acid to investigate the intracellular distribution patterns of the two different types of fatty acids. The fatty acids were again complexed to serum albumin and cells were incubated with a concentration of 400 μM each. These two fatty acids were chosen because they are different with respect to their cellular function. While arachidonic acid is bioactive and a precursor to inflammatory molecules such as prostaglandins, palmitic acid is a storage molecule and acts as a precursor for the synthesis of longer fatty acid chains. The previous analyses revealed that uptake and storage efficiency of arachidonic acid in lipid droplets compared to palmitic acid or oleic acid is quite different.

Figure 6a depicts the Raman spectrum of a lipid droplet of a cell (red) incubated for 24 h with polyunsaturated d_8-arachidonic and saturated d_{31}-palmitic acid that is overlaid by the pure spectra of d_8-arachidonic (black) and d_{31}-palmitic acid (green). Both fatty acids are stored in lipid droplets alongside each other. Because of the different types of deuterium labels of the two fatty acids (=CD vs. CD), it is possible to differentiate between the signals originating from the d_{31}-palmitic acid (2,100 and 2,197 cm^{-1}) and the one from d_8-arachidonic

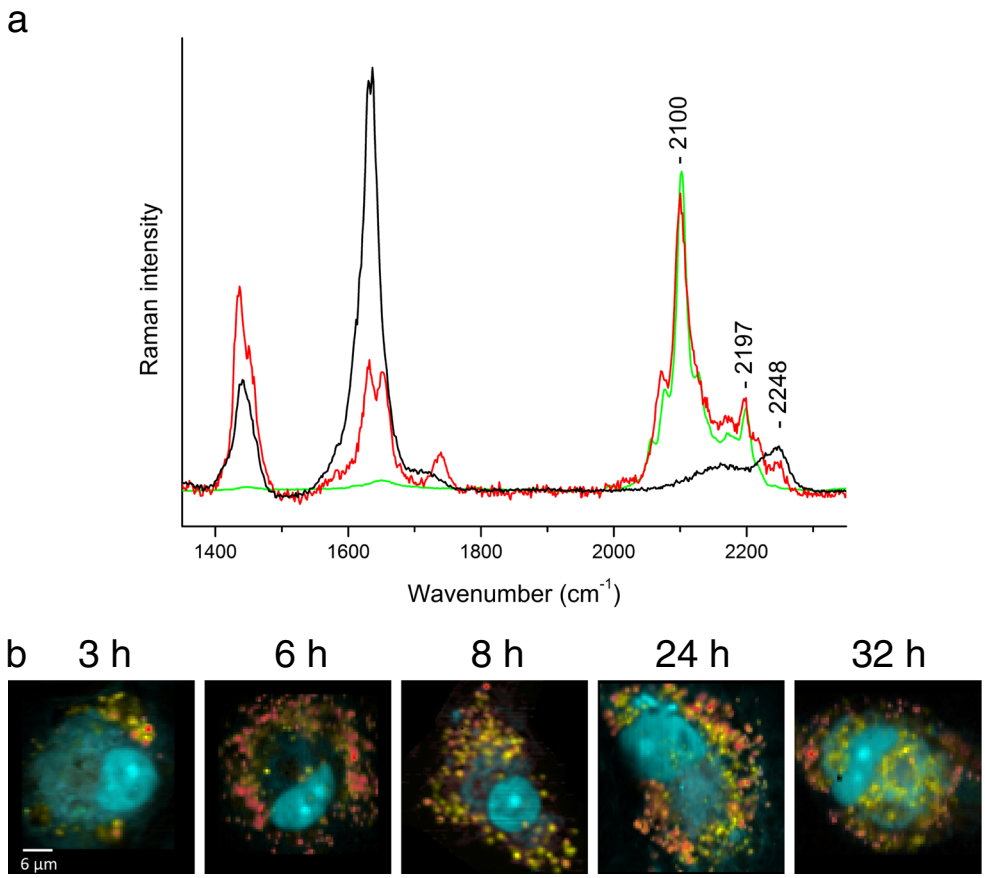

Fig. 6 **a** Raman spectrum of a lipid droplet of a cell (*red*) incubated for 24 h with both 400 μM d_8-arachidonic acid and 400 μM d_{31}-palmitic acid complexed to serum albumin overlaid by the pure spectra of d_8-arachidonic acid (*black*) and d_{31}-palmitic acid (*green*). Bands at 2,100 and 2,197 cm^{-1} in the red spectrum can be assigned to d_{31}-palmitic acid, the band at 2,248 cm^{-1} to d_8-arachidonic acid. Two bands of C=C vibrations are observed at 1,633 cm^{-1} and 1,653 cm^{-1} originating from deuterated and non-deuterated, unsaturated fatty acids as explained earlier. For better spectral resolution, a grating of 600 grooves/mm was used, leading to a spectral resolution of approximately 3 cm^{-1}. **b** Reconstructed images of THP-1 macrophages with two lipid and one protein endmember spectra for different time points. *Red* corresponds to lipid droplets which feature deuterium signals of d_8-arachidonic acid and d_{31}-palmitic acid, *yellow* to lipid droplets which only feature deuterium signals of d_{31}-palmitic acid and *cyan* displays protein density

acid (2,248 cm^{-1}). Since d_{31}-palmitic acid is deuterated at all carbon atoms along the alkyl chain, the signal is more intense than that of d_8-arachidonic acid. Furthermore, the signal originating from the =CD vibrations of the d_8-arachidonic acid is associated with a sp^2-hybridization, which exhibits less intense Raman signals compared to the sp^3-hybridized CD bonds of the d_{31}-palmitic acid.

In the presence of both fatty acids, macrophages transformed rapidly into foam cells due to the high amount of lipid droplets inside the cells (Fig. 6b). Interestingly, the storage distribution of the two fatty acids inside the same cell is not homogeneous. In the early phase of incubation, d_8-arachidonic acid is present only in a few lipid droplets. In contrast, d_{31}-palmitic acid is immediately distributed over the whole cell after starting the incubation and is detected in almost all lipid droplets within a cell independent of the incubation time. The amount of lipid droplets which feature d_8-arachidonic acid is increasing over time but not quantifiable due to high differences between cells incubated for the same time. For long incubation times higher than 24 h, the majority of lipid droplets surrounding the nucleus are comprised only by d_{31}-palmitic acid. Figure 6b exemplary shows reconstructed N-FINDR images of THP-1 macrophages incubated with the two fatty acids for different time points. On average, four endmembers for each cell were investigated (see Electronic Supplementary Material Fig. S2). Two lipid endmembers, one with both d_8-arachidonic acid and d_{31}-palmitic acid (red) and one with just d_{31}-palmitic acid (yellow), and one endmember showing the protein distribution (cyan) are depicted. The corresponding red lipid endmember spectrum shows a distinct band at 2,248 cm^{-1}, which is not detectable in the yellow endmember spectrum representing d_{31}-palmitic acid. d_8-Arachidonic acid is therefore stored in different concentrations in lipid droplets within one cell if d_{31}-palmitic acid is present. This is in contrast to its storage in all lipid droplets in the case of macrophages solely incubated with d_8-arachidonic acid.

Conclusions

In this study, we have presented the uptake and storage behavior of arachidonic acid in human macrophages. By using Raman micro-spectroscopy and deuterium-labeled arachidonic acid, we were able to trace exogenously provided arachidonic acid within cytosolic lipid droplets in macrophages. Spectral analyses revealed that the bulk of the fatty acid is not subjected to β-oxidation following uptake. This was confirmed by gas chromatography measurements, which also revealed that arachidonic acid is elongated to adrenic acid in significant amounts. Our results show that macrophages quickly store arachidonic acid in lipid droplets in case of excessive exposure. Saturation is reached after 8 h of incubation. The increased cellular accumulation of arachidonic acid after 8 h as discovered by gas chromatography in contrast to the saturation of its storage in lipid droplets suggests that in late periods of incubation the fatty acid may be stored mostly in membrane phospholipids rather than in lipid droplet storage organelles. However, our data also provide evidence that free arachidonic acid is also converted at least in part into adrenic acid by two-carbon elongation before integration into lipid droplets or phospholipids. This biologically relevant observation indicates that the immediate storage in lipid droplets after uptake may be a protective mechanism against lipotoxicity that is overwhelmed at later stages. However, the reasons for the more limited capability for storing arachidonic acid in contrast to the larger ability to store palmitic acid or oleic acid needs to be unraveled. In contrast to arachidonic acid, palmitic acid is stored predominantly in lipid droplets [19], whereas arachidonic acid may also be metabolized to phospholipids [38], which cannot be located by Raman micro-spectroscopy.

Co-supplementation studies with both fatty acids were also performed. Through their distinctive deuterium signals, we were able to distinguish their subcellular distribution in macrophages. Clear foam cell formation for long incubation times was detected and a non-homogenous storage pattern in lipid droplets is obvious. In contrast to palmitic acid, arachidonic acid is not stored homogenously in all lipid droplets.

Raman micro-spectroscopy proved to be a powerful tool to spatially resolve and investigate the chemical compositions of a single cell. This allows studying not only the distribution and quantity of lipid droplets on single cell level but also the location of exogenously provided fatty acids. As a non-destructive and non-invasive method, it also enables future in vivo studies. These are advantages compared to common methods which are based on bulk samples. However, gas chromatography provides additional chemical information as to the presence of other fatty acids in the cells such as precursors and metabolites. Only through the combination of several different methods like Raman micro-spectroscopy and gas chromatography will it be possible to fully understand the molecular processes in cells.

Acknowledgments We thank Carsten Rohrer for conducting the GC measurements, Maria Wallert and Lisa Schmölz for the introduction into the cell culture work and Dr. Iwan W. Schie for helpful discussions. We gratefully acknowledge the financial support by the Carl Zeiss Stiftung and the "Jenaer Biochip Initative 2.0" (JBCI 2.0). The project "JBCI 2.0" (03IPT513Y) within the framework "InnoProfile-Transfer–Unternehmen Region" is supported by the Federal Ministry of Education and Research (BMBF), Germany.

References

1. Lorkowski S, Cullen P (2007) Atherosclerosis: pathogenesis, clinical features and treatment. Wiley, Chichester
2. Ohsaki Y, Suzuki M, Fujimoto T (2014) Open questions in lipid droplet biology. Chem Biol 21:86–96
3. Melo RC, D'Avila H, Wan HC, Bozza PT, Dvorak AM, Weller PF (2011) Lipid bodies in inflammatory cells: structure, function, and current imaging techniques. J Histochem Cytochem 59:540–556
4. Listenberger LL, Han X, Lewis SE, Cases S, Farese RV Jr, Ory DS, Schaffer JE (2003) Triglyceride accumulation protects against fatty acid-induced lipotoxicity. Proc Natl Acad Sci U S A 100:3077–3082
5. Martins de Lima T, Cury-Boaventura MF, Giannocco G, Nunes MT, Curi R (2006) Comparative toxicity of fatty acids on a macrophage cell line (J774). Clin Sci 111:307–317
6. Diem M, Mazur A, Lenau K, Schubert J, Bird B, Miljkovic M, Krafft C, Popp J (2013) Molecular pathology via IR and Raman spectral imaging. J Biophotonics 6:855–886
7. Krafft C, Dietzek B, Popp J (2009) Raman and CARS microspectroscopy of cells and tissues. Analyst 134:1046–1057
8. Lattermann A, Matthäus C, Bergner N, Beleites C, Romeike BF, Krafft C, Brehm BR, Popp J (2013) Characterization of atherosclerotic plaque depositions by Raman and FTIR imaging. J Biophotonics 6:110–121
9. Wu H, Volponi JV, Oliver AE, Parikh AN, Simmons BA, Singh S (2011) In vivo lipidomics using single-cell Raman spectroscopy. Proc Natl Acad Sci U S A 108:3809–3814
10. Matthäus C, Dochow S, Bergner G, Lattermann A, Romeike BF, Marple ET, Krafft C, Dietzek B, Brehm BR, Popp J (2012) In vivo characterization of atherosclerotic plaque depositions by Raman-probe spectroscopy and in vitro coherent anti-stokes Raman scattering microscopic imaging on a rabbit model. Anal Chem 84:7845–7851
11. Krafft C, Neudert L, Simat T, Salzer R (2005) Near infrared Raman spectra of human brain lipids. Spectrochim Acta A Mol Biomol Spectrosc 61:1529–1535
12. Neugebauer U, Bocklitz T, Clement JH, Krafft C, Popp J (2010) Towards detection and identification of circulating tumour cells using Raman spectroscopy. Analyst 135:3178–3182
13. Dochow S, Krafft C, Neugebauer U, Bocklitz T, Henkel T, Mayer G, Albert J, Popp J (2011) Tumour cell identification by means of Raman spectroscopy in combination with optical traps and microfluidic environments. Lab Chip 11:1484–1490
14. Hedegaard M, Krafft C, Ditzel HJ, Johansen LE, Hassing S, Popp J (2010) Discriminating isogenic cancer cells and identifying altered unsaturated fatty acid content as associated with metastasis status, using k-means clustering and partial least squares-discriminant analysis of Raman maps. Anal Chem 82:2797–2802
15. Chan JW (2013) Recent advances in laser tweezers Raman spectroscopy (LTRS) for label-free analysis of single cells. J Biophotonics 6:36–48
16. Kirchner SR, Ohlinger A, Pfeiffer T, Urban AS, Stefani FD, Deak A, Lutich AA, Feldmann J (2012) Membrane composition of jetted lipid vesicles: a Raman spectroscopy study. J Biophotonics 5:40–46
17. Matthäus C, Schubert S, Schmitt M, Krafft C, Dietzek B, Schubert US, Popp J (2013) Resonance Raman spectral imaging of intracellular uptake of beta-carotene loaded poly(D, L-lactide-co-glycolide) nanoparticles. ChemPhysChem 14:155–161
18. Schie IW, Nolte L, Pedersen TL, Smith Z, Wu J, Yahiatene I, Newman JW, Huser T (2013) Direct comparison of fatty acid ratios in single cellular lipid droplets as determined by comparative Raman spectroscopy and gas chromatography. Analyst 138:6662–6670
19. Matthäus C, Krafft C, Dietzek B, Brehm BR, Lorkowski S, Popp J (2012) Noninvasive imaging of intracellular lipid metabolism in macrophages by Raman microscopy in combination with stable isotopic labeling. Anal Chem 84:8549–8556
20. Caruso D, Rise P, Galella G, Regazzoni C, Toia A, Galli G, Galli C (1994) Formation of 22 and 24 carbon 6-desaturated fatty acids from exogenous deuterated arachidonic acid is activated in THP-1 cells at high substrate concentrations. FEBS Lett 343:195–199
21. Slipchenko MN, Le TT, Chen H, Cheng JX (2009) High-speed vibrational imaging and spectral analysis of lipid bodies by compound Raman microscopy. J Phys Chem B 113:7681–7686
22. Brash AR, Ingram CD (1986) Lipoxygenase metabolism of endogenous and exogenous arachidonate in leukocytes: GC-MS analyses of incubations in H2(18)O buffers. Prostaglandins Leukot Med 23:149–154
23. Gazi E, Harvey TJ, Brown MD, Lockyer NP, Gardner P, Clarke NW (2009) A FTIR microspectroscopic study of the uptake and metabolism of isotopically labelled fatty acids by metastatic prostate cancer. Vib Spectrosc 50:99–105
24. Gazi E, Gardner P, Lockyer NP, Hart CA, Brown MD, Clarke NW (2007) Direct evidence of lipid translocation between adipocytes and prostate cancer cells with imaging FTIR microspectroscopy. J Lipid Res 48:1846–1856
25. Brash AR (2001) Arachidonic acid as a bioactive molecule. J Clin Invest 107:1339–1345
26. Spector AA (1999) Essentiality of fatty acids. Lipids 34(Suppl):S1–S3
27. Perez R, Matabosch X, Llebaria A, Balboa MA, Balsinde J (2006) Blockade of arachidonic acid incorporation into phospholipids induces apoptosis in U937 promonocytic cells. J Lipid Res 47:484–491
28. van Manen HJ, Kraan YM, Roos D, Otto C (2005) Single-cell Raman and fluorescence microscopy reveal the association of lipid bodies with phagosomes in leukocytes. Proc Natl Acad Sci U S A 102:10159–10164
29. Schnoor M, Cullen P, Lorkowski J, Stolle K, Robenek H, Troyer D, Rauterberg J, Lorkowski S (2008) Production of type VI collagen by human macrophages: a new dimension in macrophage functional heterogeneity. J Immunol 180:5707–5719
30. Schnoor M, Buers I, Sietmann A, Brodde MF, Hofnagel O, Robenek H, Lorkowski S (2009) Efficient non-viral transfection of THP-1 cells. J Immunol Methods 344:109–115
31. Winter ME (1999) N-FINDR: an algorithm for fast autonomous spectral end-member determination in hyperspectral data. Proc SPIE 3753:266–275
32. Hedegaard M, Matthäus C, Hassing S, Krafft C, Diem M, Popp J (2011) Spectral unmixing and clustering algorithms for assessment of single cells by Raman microscopic imaging. Theor Chem Acc 130:1249–1260
33. Boelens HF, Dijkstra RJ, Eilers PH, Fitzpatrick F, Westerhuis JA (2004) New background correction method for liquid chromatography with diode array detection, infrared spectroscopic detection and Raman spectroscopic detection. J Chromatogr A 1057:21–30
34. Bligh EG, Dyer WJ (1959) A rapid method of total lipid extraction and purification. Can J Biochem Physiol 37:911–917
35. Kraft J, Collomb M, Mockel P, Sieber R, Jahreis G (2003) Differences in CLA isomer distribution of cow's milk lipids. Lipids 38:657–664
36. Chan JW, Motton D, Rutledge JC, Keim NL, Huser T (2005) Raman spectroscopic analysis of biochemical changes in individual triglyceride-rich lipoproteins in the pre- and postprandial state. Anal Chem 77:5870–5876
37. Comai K, Farber SJ, Paulsrud JR (1975) Analyses of renal medullary lipid droplets from normal, hydronephrotic, and indomethacin treated rabbits. Lipids 10:555–561
38. Guijas C, Astudillo AM, Gil-de-Gomez L, Rubio JM, Balboa MA, Balsinde J (2012) Phospholipid sources for adrenic acid mobilization in RAW 264.7 macrophages. Comparison with arachidonic acid. Biochim Biophys Acta 1821:1386–1393